AN IN-SITU INVESTIGATION OF THE SOLUBILITY OF MOLYBDENUM TRIOXIDE IN OXYGENATED WATER AT SUPERCRITICAL CONDITIONS

P. R. Meredith[1], A. J. Anderson[1], and R.A. Mayanovic[2]
[1] St. Francis Xavier University, Antigonish, Nova Scotia, Canada
[2] Missouri State University, Springfield, Missouri, U.S.A.

Abstract

The solubility of MoO_3 in a 1M H_2O_2 aqueous solution was investigated under supercritical conditions in a hydrothermal diamond anvil cell (HDAC). Quantitative analyses of the aqueous solution in equilibrium with a crystal of MoO_3 were obtained at 400, 450 and 500 ºC and pressures of 44, 75, and 113 MPa respectively using micro synchrotron x-ray fluorescence (μSXRF). The μSXRF spectra were collected at the Pacific Northwest Consortium (PNC) x-ray microprobe facility at the Advanced Photon Source, Argonne National Laboratory. It was found that the solubility of MoO_3 in water above the critical point is higher than previously reported.

1. Introduction

Molybdenum is a group VI transition metal with a complex chemistry stemming from the wide range of possible oxidation states (-2 to +6), the ability to form polynuclear complexes, and coordination numbers ranging from 4 to 8. Molybdenum is found in nature primarily as the molybdenum (IV) sulphide mineral molybdenite (MoS_2). Occasionally Mo manifests in the Earth's crust, in association with oxidation zones of Mo deposits, as the molybdenum (VI) oxide molybdite (MoO_3) and is very rarely found as the molybdenum (IV) oxide, tugarinovite (MoO_2).

The elemental properties of high melting point and low coefficient of thermal expansion transfer upon alloying and the addition of molybdenum enhances the tensile strength and chemical durability of steel. Such molybdenum-bearing high strength steel alloys are among the candidate materials to be used in the construction of supercritical water cooled nuclear reactors.
The Gen IV supercritical water cooled reactors (SCWR) are designed to function at temperatures ranging from 250 to 625°C and pressures ranging from 25 to 30 MPa [1]. However, the successful deployment and operation of Gen IV reactors will depend on the ability to predict and control water chemistry under extreme conditions of radiation and temperature. A primary concern, with regard to candidate materials, is the potential for, and magnitude of, corrosion product transport in supercritical water [1]. Previous hydrothermal experiments have shown that a significant amount of Mo from the walls of HastelloyC and Alloy 625 autoclaves is dissolved in pure water at 450 °C after 280 hours [1].

The solubility of Mo in various aqueous solutions and vapours from ambient temperature up to 800 °C has been investigated [2,3,4,5,6]. However, with the exception of [2], the solubility estimates were determined by analyzing the solutions after quenching to room temperature.

In the present study, a Bassett-type hydrothermal diamond anvil cell (HDAC) was used to directly measure the solubility of MoO_3 in supercritical water. An aqueous solution in

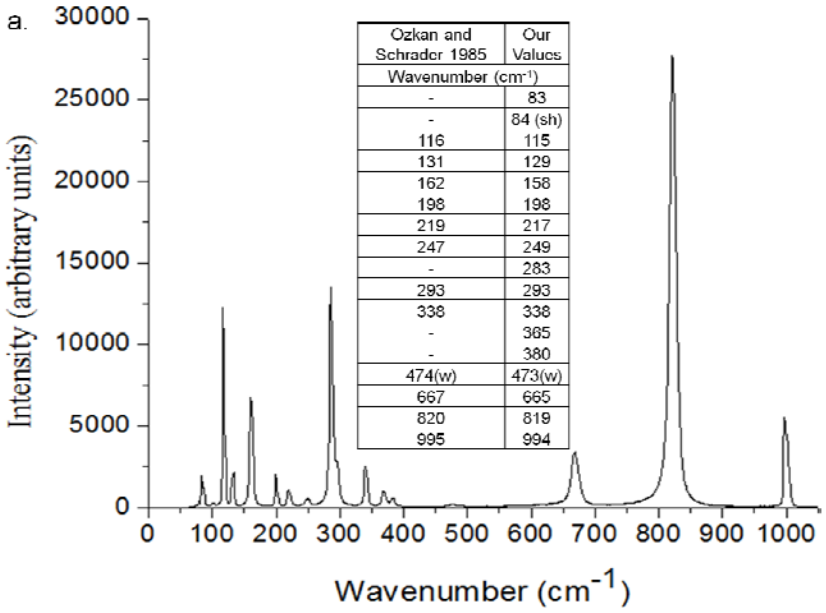
equilibrium with a MoO_3 crystal at high temperature and pressure was separately analyzed using micro synchrotron x-ray fluorescence (μSXRF). These in situ measurements eliminate analytical inaccuracies related to the precipitation and crystal growth from solution during quenching. Unlike previous hydrothermal diamond anvil cell experiments [7, 8], a recess in one of the diamond anvils, instead of a metal gasket, is used as the sample chamber. Lack of a metal gasket eliminates volume changes caused by gasket deformation, reduces the potential for diamond dissolution and the production of carbon species (i.e. CO_2, CH_4), and eliminates contamination of fluid by the gasket material [9].

2. Experimental procedure

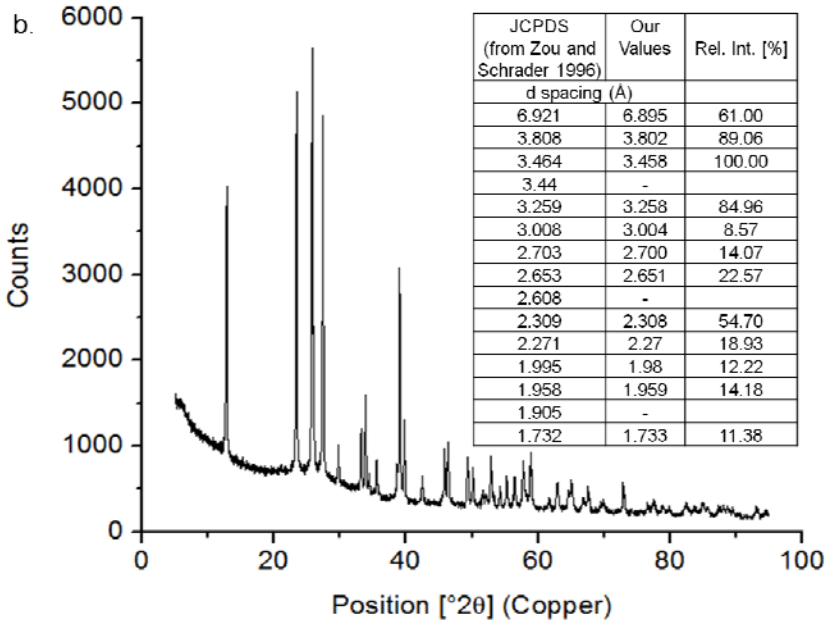
2.1 Synthesis and characterization of starting materials

Single crystals of molybdite (MoO_3) were prepared through sublimation of commercially available molybdenum(VI) oxide powder (99.99+%, CAS 1313-27-5, GFS) in a capped ceramic crucible at 700 °C for 30 minutes. The crystals produced were identified as molybdite using Raman spectra obtained with a Renishaw InVia Raman microscope and by powder x-ray diffraction (XRD) patterns obtained using a Panalytical X-pert pro diffractometer (Figure 1).

Solutions of 1 M H_2O_2 were prepared before each experiment by the dilution of 35 wt% H_2O_2 with deoxygenated deionised water. The pH of each freshly prepared 1M H_2O_2 solution was 5.5.



Ozkan and Schrader 1985	Our Values
Wavenumber (cm^{-1})	
-	83
-	84 (sh)
116	115
131	129
162	158
198	198
219	217
247	249
-	283
293	293
338	338
-	365
-	380
474(w)	473(w)
667	665
820	819
995	994



JCPDS (from Zou and Schrader 1996)	Our Values	Rel. Int. [%]
d spacing (Å)		
6.921	6.895	61.00
3.808	3.802	89.06
3.464	3.458	100.00
3.44	-	
3.259	3.258	84.96
3.008	3.004	8.57
2.703	2.700	14.07
2.653	2.651	22.57
2.608	-	
2.309	2.308	54.70
2.271	2.27	18.93
1.995	1.98	12.22
1.958	1.959	14.18
1.905	-	
1.732	1.733	11.38

Figure 1 Representative Raman spectrum of synthetic MoO_3 crystals (a), and powder XRD pattern of synthetic MoO_3 crystals referenced to [10] (b)

2.2 Hydrothermal Diamond Anvil Cell (HDAC)

All solubility experiments were conducted in a Bassett-type HDAC [11, 12]. Previous publications provide a detailed description of the HDAC [11, 12], thus, only a brief description is given here.

The HDAC is a reaction vessel designed for the purpose of studying fluids and fluid-solid interactions over a wide range of temperatures and pressures. The cell consists of two opposing stainless steel platens which fit together through the use of three guide posts. At the center of each platen is a diamond anvil which is mounted onto a tungsten carbide (WC) seat. The WC seats are wound with Chromel wire (Ni20Cr80, 0.010", Omega), which provide heat to the diamond anvils when a voltage is applied. To avoid destructive oxidation of components within the cell at high temperatures, a stainless steel sleeve, through which inert Ar gas is pumped, is fitted around the cell.

A U-shaped sample chamber was laser milled into the culet face of one of the diamond anvils (Figure 5). The depth of the sample chamber is approximately 30 μm. A gold barrier was inserted into a small trench (50 μm wide) between the arms of the U-shaped recess, in order to prevent the excitation and detection of the MoO_3 crystal by scattered x-rays in the diamond anvil.

Loading of the HDAC consists of first transferring a small crystal of MoO_3 into the recess using a fine bristle. Aqueous solution is then added to the recess before quickly sealing the sample chamber by drawing the diamond anvils together. In order to minimize the diffusion of any gases into or out of the aqueous solution during loading, solutions are exposed to the surrounding air for no more than 30 seconds.

The temperature of the system was monitored using K-type (Alumel-Chromel) thermocouples and controlled using a Linkam™ programmable temperature controller. The instrument was calibrated using pure water synthetic fluid inclusions (homogenization = 374 °C), the alpha-beta phase transition of quartz (573 °C), and the melting point of pure NaCl (801°C). The temperature of both diamonds was held to within 0.1°C of each other over the entire temperature range of the experiment. A transmitting light microscope with video attachment was used to view the sample in real time and record each experiment. Figure 2 shows a simplified block diagram of a HDAC after the sample (MoO_3 + solution) is enclosed.

Observing the temperature of liquid to vapour homogenization (i.e. liquid + vapour → liquid) is imperative to ensuring the sample contents have not leaked during an experiment. The temperature of liquid to vapour homogenization (T_H) is recorded while bringing the system to high temperature and again during cooling. No change in the liquid-vapour homogenization temperature, measured before and after the fluid sample was held at the maximum temperature and pressure of the experiment, indicates that partial leakage of the fluid did not occur and that a constant density was maintained.

The density of the aqueous fluid after sealing the HDAC was determined using the $T_{H,}$ and the pressure at a given temperature was calculated using the equation of state (EOS) for water [13]. However, due to changes in chemistry of the system as more MoO_3 is dissolved, the system cannot be accurately treated as a pure water system. Hence, the estimated pressure will deviate slightly from that of a pure water system over the temperature range studied. In a NaCl-H_2O system containing 2 wt% NaCl at the same conditions as experiments conducted in this study, pressure only exceeds that of a pure water system by ~ 11MPa at 500 °C. The EOS of Mo-bearing fluids is not known, therefore, to precisely measure the pressure at a given temperature, a pressure calibrant, such as quartz [14], must be added to the MoO_3-H_2O system. The oxygen fugacity conditions were imposed by the 1M H_2O_2 fluid. Based on the sudden appearance of MoO_2 at temperatures of about 610 °C we estimate the log fO_2 in the sample chamber to be about -9 [15]. Assuming the total decomposition of H_2O_2 to H_2O and O_2, this aqueous solution can be treated as pure H_2O.

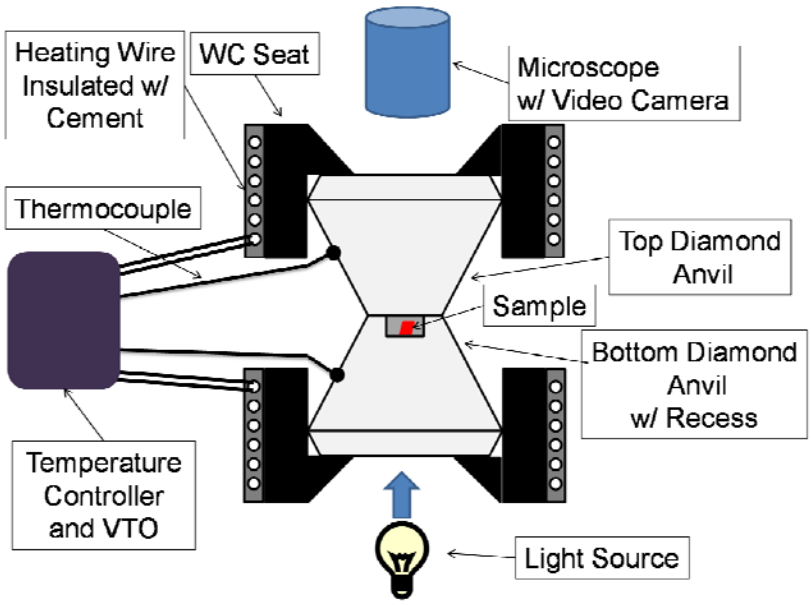


Figure 2 A schematic diagram of the hydrothermal diamond anvil cell with sample

2.3 Synchrotron x-ray fluorescence analysis

Quantitative micro synchrotron x-ray fluorescence (μSXRF) analysis of the aqueous solution in the HDAC was performed at the Pacific Northwest Consortium x-ray microprobe facility at the Advanced Photon Source (APS), Argonne National Laboratory. The experimental configuration is shown in Figure 3. A 20.2 keV x-ray beam having a flux of about 1×10^{11} photons/sec was focussed to a spot size of about 5 x 5 μm. The path of the x-ray microbeam through the U-shaped sample chamber is shown in figure 5. Visible fluorescence of the x-rays through the diamond anvil allowed for the precise positioning of the beam in the sample chamber. The MoO_3 crystal, located on the opposite side of the sample chamber, was effectively shielded from the detector and scattered x-rays by the gold barrier.

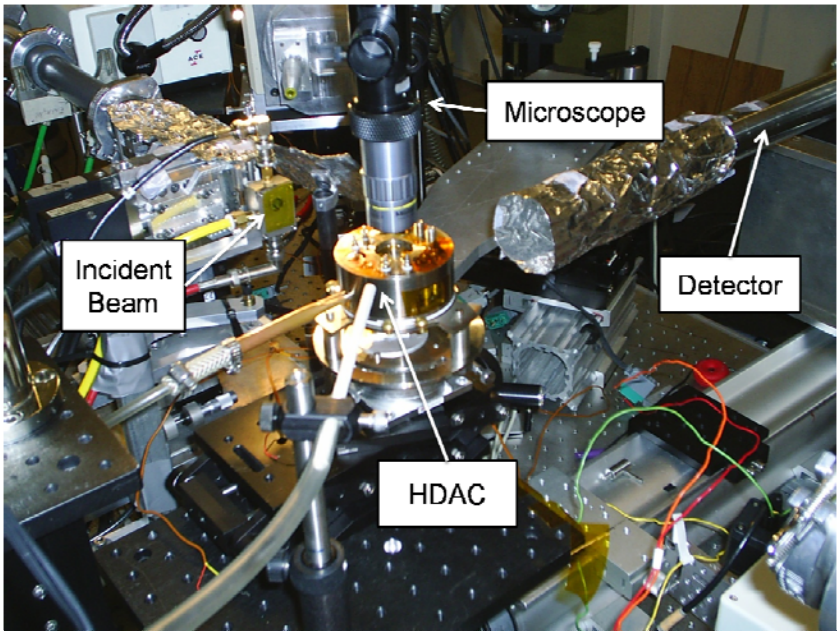


Figure 3 Experimental configuration

The μSXRF spectra were collected for a period of 60 seconds using a Peltier-cooled Vortex ME4 four element detector. Standardization was performed using standard solutions containing 1,000, 2,500, 5,000, 7,500, and 10,000 mg/L Mo. Stock 1,000 mg/L Mo and 10,000 mg/L Mo were obtained from Fluka Analytical and GFS Chemicals, respectively. Intermediate concentrations were prepared by diluting the 10,000 mg/L stock with deionised water. Figure 4 shows the linear calibration curves for different standard solutions in the HDAC. The percent relative uncertainty of the measured Mo concentrations using μSXRF and the HDAC is 2%.

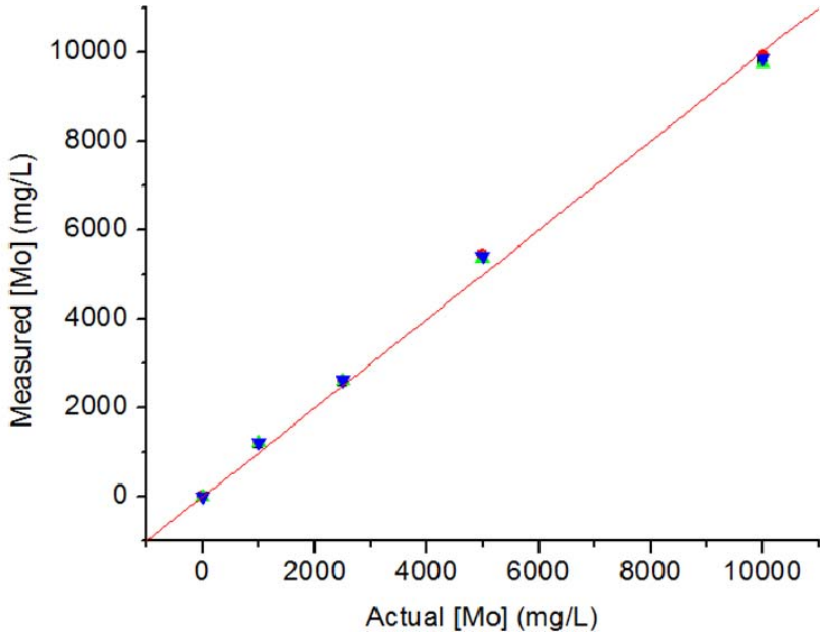


Figure 4 Mo standard solution calibration curves in the HDAC

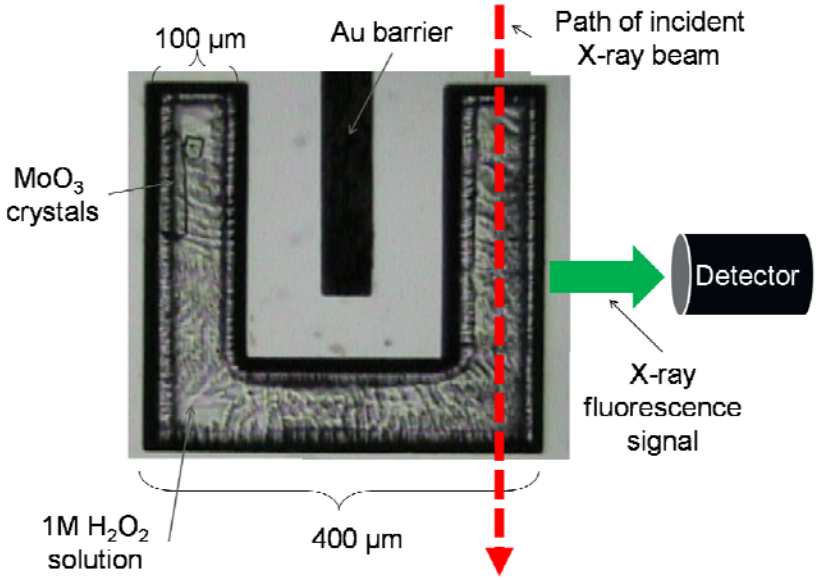


Figure 5 Photograph of the U-shaped sample chamber showing the location of the MoO_3 crystal and the X-ray beam path

Spectra were collected after the system was held at the selected temperature for a period of 30 minutes. All experiments indicate that there was no noticeable change in the size of the MoO_3 crystal after 30 minutes. Equilibrium conditions were investigated by increasing or decreasing temperature slightly (~ 1 °C). In response to this slight temperature fluctuation, the crystal of MoO_3 would shrink or grow quickly. Extended irradiation of the solution above 400 °C resulted in a slight yet noticeable decrease in Mo counts; possibly due to radiolysis-induced precipitation of Mo oxide particles. This decrease in Mo counts corresponds to approximately 10 to 20 ppm over the three acquisitions. In order to minimize the radiolysis of the solution only three spectra were acquired at each temperature. All µSXRF data were analyzed using GeoPIXE II spectral analysis software (© CSIRO).

3. Results

Synchrotron x-ray fluorescence spectra obtained from the solution equilibrated with a crystal of MoO_3 at 400, 450, and 500 °C are shown in figure 6. The calculated Mo concentrations in solution at different temperature and pressure conditions are given in Table 1. The density of H_2O was determined from the observed liquid-vapour homogenization temperature.

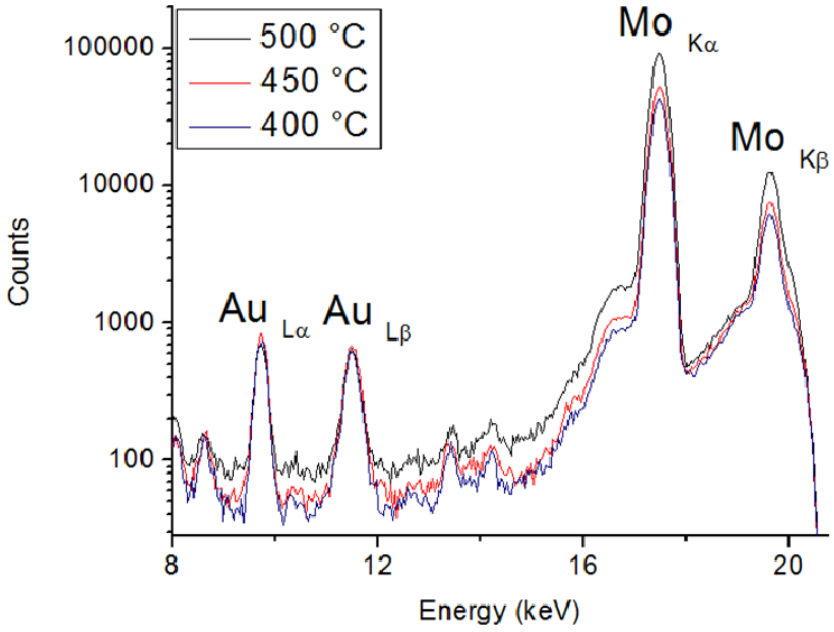


Figure 6 μSXRF spectra of aqueous solution containing MoO_3 in the hydrothermal diamond anvil cell at 400, 450 and 500 ºC

Experiment #	T (°C)	$T_{H(L+V=>L)}$	P (MPa)	ρ (g/cm^3)	[Mo] (mg/L)	[Mo] (*m*)
5	500	352.9	113	0.562	8595 ± 134.0	5.035E-02 ± 7.852E-04
6	400	355.9	44.0	0.549	3995 ± 12.91	2.263E-02 ± 7.387E-05
6	450	355.9	75.5	0.549	4921 ± 40.31	2.805E-02 ± 2.307E-05
7	500	352.8	114	0.563	8663 ± 59.09	5.083E-02 ± 3.468E-04

Table 1 The concentration of Mo in solution at 400, 450 and 500 °C

4. Discussion

The solubility of MoO_3 in pure water has been investigated by Ivanova et al. [3], Gong et al. [16], and Ulrich and Mavrogenes [2]. Ivanova et al. performed dissolution experiments at vapour saturation pressures at 150, 175, 200, 250, and 300 °C in Ti-autoclaves. The aqueous solutions in the autoclaves were analyzed colorimetrically after quenching. Neither pH nor oxygen fugacity was buffered in their experiments. Gong et al. [16] used cold-seal pressure vessels to measure the solubility of MoO_3 at 417 °C at pressures between 29 and 150 MPa. Ulrich and Mavrogenes [2] measured the solubility of Mo in solutions trapped as synthetic quartz-hosted fluid inclusions at 200 MPa and temperatures from 500 to 800 °C. The individual fluid inclusions were analyzed by laser ablation inductively coupled plasma mass spectrometry (LA-ICPMS). The experiments were redox-buffered using Ni/NiO or Re/ReO_2 plus water and the pH was buffered using an assemblage of muscovite, K-feldspar and quartz.

Figure 7 compares the Mo solubility measurements from this study with the results from previous MoO_3-H_2O experiments. Only one measurement by Gong et al. [16] taken at 417 ºC and 55 MPa is presented because the pressure and fluid density most closely matches our experimental conditions at 400 ºC.

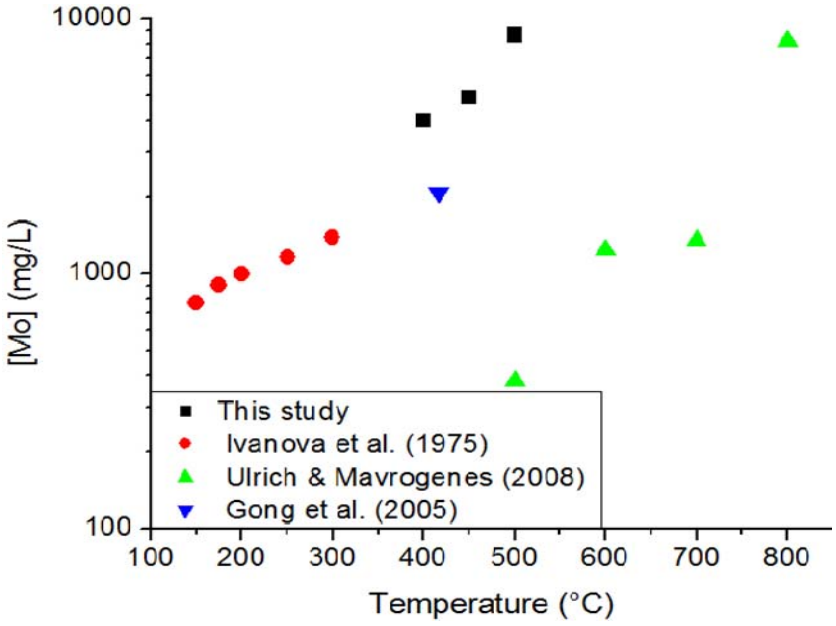


Figure 7 Experimental Mo solubilities in the MoO_3-H_2O system

Although previous experimental studies indicate that MoO_3 solubility increases with temperature and pressure in the supercritical region, there is significant disagreement in the reported absolute concentrations of Mo in supercritical water. The solubility of MoO_3 measured in this study at 500 ºC and 113 MPa is an order of magnitude higher than that of Ulrich and Mavrogenes at 500 ºC and 200 MPa. This discrepancy is not due to the lower pressure conditions employed in our study because the solubility of MoO_3 in pure water is expected to increase with pressure [16]. Our measurements at 400 ºC are in broad agreement with Gong et al. [16]. The higher solubility behaviour reported here can be attributed in part to the higher $fO2$ conditions employed but could also be due to partial precipitation of Mo during quenching in the experiments of Gong et al.

Knowledge of transition metal solubility and speciation at extreme conditions of temperature and radiation is needed to better predict corrosion product transport and deposition in GEN IV systems. A 1 M H_2O_2 solution was used in this study to increase the $fO2$ of the system in order to inhibit the precipitation of MoO_2 at high temperatures. In the context of nuclear power, it is important understand how H_2O_2, a product of the decomposition of water by radiolysis, may effect MoO_3 solubility.

In the course of the µSXRF analyses, it was found that prolonged x-ray irradiation of the fluid resulted in a reduction in Mo counts. This reduction is probably due to radiation-induced precipitation of Mo oxide crystals. Accordingly, it is important to minimize the exposure time of

sample at the desired temperature by collecting x-ray spectra for very short periods of time. The HDAC should be reloaded with fresh starting materials for measurements at a different temperature.

5. Conclusions

In agreement with previous studies, our results indicate that the solubility of MoO_3 increases with temperature and pressure in the supercritical region. Furthermore, the high solubility of MoO_3 at 500 ºC and 113 MPa (8,600 mg/L) corroborate the solubility behaviour reported by Gong et al. [16] and demonstrate the potential for Mo mobility in supercritical water reactors. The results also show the advantages of the HDAC-μSXRF method for solubility studies of transition metal oxide-supercritical water systems.

6. Acknowledgments

NSERC/NRCan/AECL Generation IV Energy Technologies Program is acknowledged for funding through a NSERC Collaborative Research and Development (CRD) grant. R.A.M. was funded as part of the EFree, an Energy Frontier Research Center, funded by the US DOE (DE-SC0001057). PNC/XOR facilities at the Advanced Photon Source, and research at these facilities, are supported by the US Department of Energy - Basic Energy Sciences, a Major Resources Support grant from NSERC, the University of Washington, Simon Fraser University and the Advanced Photon Source. Use of the Advanced Photon Source is also supported by the U. S. Department of Energy, Office of Science, Office of Basic Energy Sciences, under Contract DE-AC02-06CH11357.

7. References

[1] D. Guzonas, P. Tremaine, J-P. Jay-Gerin, "Chemistry control challenges in a supercritical water cooled reactor", International Conference on Water Chemistry of Nuclear Reactor Systems (NPC'08) in Berlin, September 15-18, 2008

[2] T. Ulrich, J. Mavrogenes, "An experimental study of the solubility of molybdenum in H_2O and KCl-H_2O solutions from 500 °C to 800 °C, and 150 to 300 MPa", Geochimica et Cosmochimica Acta, Vol. 72, 2008, pp. 2316-2330

[3] G.F. Ivanova, N.I. Lavkina, L.A. Nesterova, A.P. Zhudikova, I.L. Khodakovskiy, "Equilibrium in the MoO_3-H_2O system at 25-300 °C", Geochemistry International, Vol. 12, 1975, pp. 163-176

[4] K.U. Rempel, A.E. William-Jones, A.A. Migdisov, "The solubility of molybdenum dioxide and trioxide in HCl-bearing water vapour at 350 °C and pressures up to 160 bars", Geochimica et Cosmochimica Acta, Vol. 72, 2008 pp. 3074-3083

[5] K.U. Rempel, A.E. William-Jones, A.A. Migdisov, "The partitioning of molybdenum(VI) between aqueous liquid and vapour at temperatures up to 370°C", Geochimica et Cosmochimica Acta, Vol. 73, 2009, pp.3381-3392

[6] K.U. Rempel, A.A. Migdisov, A.E. William-Jones, "The solubility and speciation of molybdenum in water vapour at elevated temperatures and pressures: implications for ore genesis", Geochimica et Cosmochimica Acta, Vol. 70, 2006, pp. 687-696

[7] W.A. Bassett, A.J. Anderson, R.A. Mayanovic, I.-M. Chou, "Modified hydrothermal diamond anvil cells for XAFS analyses of elements with low energy absorption edges in aqueous

solutions at sub- and supercritical conditions", Zeitschrift fur Kristallographie, Vol. 215, 2000, pp.711-717

[8] C. Schmidt, K. Rickers, D.H. Bilderback, R. Huang, "In situ synchrotron-radiation XRF study of REE phosphate dissolution in aqueous fluids to 800 °C", Lithos, Vol. 95, 2007, pp.87-102

[9] I-M. Chou, A.J. Anderson, "Diamond dissolution and the production of methane and other carbon-bearing species in hydrothermal diamond anvil cells", Geochimica et Cosmochimica Acta, Vol. 73, 2009, pp. 6360-6366

[10] J. Zou, G.L. Schrader, "Multicomponent thin film molybdate catalysts for the selective oxidation of 1,3-butadiene", Journal of Catalysis, Vol. 161, 1996, pp. 667-686

[11] W.A. Bassett, A.H. Shen, M.J. Bucknam, I-M. Chou, "A new diamond anvil cell for hydrothermal studies to 2.5 GPa and -190 °C to 1200 °C", Rev. Sci. Instrum. Vol. 64, 1993, pp.2340-2345

[12] W.A. Bassett, "High pressure-temperature aqueous systems in the hydrothermal diamond anvil cell (HDAC)", Eur. J. Mineral, Vol. 15, 2003, pp.773-780

[13] W. Wagner, A. Pruss, "The IAPWS formulation 1995 for the thermodynamic properties of ordinary water substance for general and scientific use", J. Phys. Chem. Ref. Data, Vol. 31, 2002, pp.387-535

[14] C. Schmidt, M.A. Ziemann, "In-situ Raman spectroscopy of quartz: a pressure sensor for hydrothermal diamond-anvil cell experiments at elevated temperatures", American Mineralogist, Vol. 85, 2000, pp.1725-1734

[15] Y. Xiong, S.A. Wood, "Experimental determination of the solubility of ReO_2 and the dominant oxidation state of rhenium in hydrothermal solutions", Chemical Geology, Vol. 158, 1999, pp. 245-256

[16] Q.J. Gong, C.W. Yu, K. Cen, Y.R. Wang, 'Experimental determination of MoO_2 and WO_3 solubilities in supercritical fluids", Acta Petrologica Sinica, Vol. 21, 2005, pp.240-244